INTERFACIAL MICROMECHANICS AND EFFECT OF MOISTURE ON FLUORINATED EPOXY CARBON FIBER COMPOSITES

By

CHIRAG H. KARELIYA

Bachelor of Engineering in Mechanical Engineering
University of Mumbai
Mumbai, India
2005

Submitted to the Faculty of the
Graduate College of
Oklahoma State University
in partial fulfillment of
the requirements for
the Degree of
MASTER OF SCIENCE
December, 2009

INTERFACIAL MICROMECHANICS AND EFFECT OF MOISTURE ON FLUORINATED EPOXY CARBON FIBER COMPOSITES

Thesis Approved:

Dr. Raman P. SIngh

Thesis Advisor

Dr. Jay C. Hanan

Dr. Sandip P. Harimkar

Dr. A. Gordon Emslie

Dean of the Graduate College

ACKNOWLEDGMENTS

It's been a roller coaster ride pursuing my master's degree here at oklahoma state university filled with lows, highs as well as plateaus. Lows characterized by moments of failures in research or bad grades in classes, highs full of progress in a small yet important and challenging steps in research, and plateaus characterized by everyday life. However, this roller coaster ride was made less daunting and more joyful due to the continued support and kindness I received from my research advisor, Dr. Raman P. Singh. I am very thankful to him for everything.

I would like to thank Dr. Jay Hanan and Dr. Kaan Kalkan for being in my thesis committee as well as Dr. Sandip Harimkar for pitching in my thesis committee at such a short notice. Discussions with Dr. Kalkan helped me many a times to think about a problem from a different perspective and thus tackling it in the process.

I am thankful to Mr. Mike Lucas at the physics instrument shop who helped my designs materialize into prototypes in very short times. I am also thankful to Mr. John Gage, and Brittani Vickers of Design and Manufacturing laboratory for their help with fabricating fixture components.

I am also thankful to Dr. Jeffrey Hinkley at the Applied Materials and Processing Branch, NASA LaRC, the NASA EPSCoR program and the Oklahoma NASA EPSCoR office for a Research Initiation Grant for funding this research which also served as my thesis project.

I would like to express my gratitude towards my very good friends/ lab-mates Arif Rahman (the dudette) and Dhivakar Jeevan Kumar (the genius2) for their friendship and support. I am also thankful to Abhishek Singh (... vo vaali movie dekhe ho?), Suraj Zunjarrao (the gameboy) and Dr. Gajendra Pandey (what, what, what ... good, good, good) for acting as my mentors. I am also thankful to my colleagues at MAML, Abhisek Bhadra (the genius1) , Abhishek Jain (the guy who loves to take his own photos, lots of them!), Andrew Byrd, Balaji Ramanujakannan (the story teller), Bradley Chai, Chaitanya Viswanadha (chatty, they closed the shutter and started ...), Kunal Mishra, (the standup comedian), Leila FJ, Matt Duncan, Mohammed Husien (a bro who is simply out of this world), Philip Rogers (the tailgate dude), and Vasudevan Rajagopalan (everybody's afraid of Vasu!).

I would also like to thank all my friends here at Stillwater whose friendship and affection made Stillwater a home away from home.

Finally, I would like to thank my parents, my brother, my bhabhi, my sister, and my jiju for their unwilling love and support without whom I would not have reached this stage!!!

TABLE OF CONTENTS

LIST OF TABLES

Table Page

LIST OF FIGURES

CHAPTER 1

Introduction

Problem Statement

Carbon fiber composite materials possess very high specific strength and stiffness. They can be engineered to specific applications due to their directional properties along the reinforcements. These characteristics make carbon fiber reinforced polymer matrix composites ideal candidates for use in aerospace structures and other mobile applications where weight is as important as the strength. For instance, the new Airbus A350 XWB has 53% composites by weight used in its structure whereas composites comprise about 50% by weight of the Boeing 787 Dreamliner as shown in figures 1.1(a), 1.1(b) and 1.2 [1, 2].

Unlike steel and aluminum, carbon fiber composites are relatively new materials and have not been studied as much for their long term durability. Hence, this increased application is also accompanied with a greater concern about their long term durability. The long term durability of carbon fiber reinforced polymer matrix composites is especially important for safety critical applications like aerospace structures which are often exposed to different environments like moisture, temperature, and UV (ultraviolet) radiation. Such environments can cause synergistic degradation of the bulk matrix, the reinforcement and most importantly, the interface. The environmental degradation of the interface directly affects load transfer mechanisms in the composite and eventually results in poor long term durability.

As a means to develop environmentally resistant composite systems, scientists at the NASA

(a) Airbus A350 XWB carbon fiber composite fuselage

(b) Boeing 787 Dreamliner carbon fiber composite fuselage

Figure 1.1: Use of carbon fiber composites as structural materials for new age commercial aircrafts.

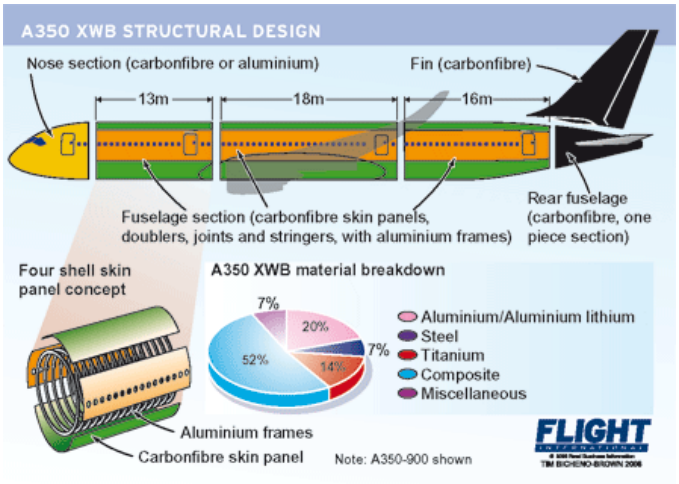

Figure 1.2: Airbus A350 XWB material breakdown [2].

Langley Research Center have synthesized a fluorinated epoxy that exhibits reduced moisture absorption. Due to this reduction in moisture absorption, such fluorinated epoxies are expected to have an increased resistance to environmental degradation and hence potentially improved long term durability. The focus of this research is to investigate the interfacial shear strength between carbon fibers and such epoxies as a function of exposure to environmental degradation by employing the microbond technique.

Environmental Degradation of Composites

Fiber reinforced polymer matrix composites are exposed to multiple environments like moisture, UV radiation, thermal cycling in numerous applications such as marine, aerospace and automotive. When exposed to such environments, these composite materials undergo complex physiochemical degradation, which not only affect the reinforcements and the matrix but also the fiber-matrix interface [3–6].

The conventional epoxies used as a matrix in fiber reinforced composites readily absorb moisture in humid environments [7, 8]. Diffusion of moisture in the epoxy matrix causes external plasticization of the epoxy [3, 9, 10]. The absorbed moisture also leads to hydrolysis of the matrix, thus affecting the physical, mechanical and chemical properties of the composite [11–13]. Perhaps, the highly polar nature of the tetraglycidyl-4,4'-methylene dianiline (TGMDA)/ diamino diphenyl sulfone (DDS) epoxy systems make them more vulnerable to moisture uptake as shown in figure 1.3. Plasticization and hydrolysis reduce the glass transition temperature of the epoxy thus affecting all the matrix dominated properties of the composite including the off axis tensile strength, compressive strength, and interlaminar shear strength. Plasticization affects the composite properties only temporarily, whereas hydrolysis causes permanent deterioration since it directly affects the chemical

bonds in the matrix and at the fiber–matrix interface [14–19].

Furthermore, in the presence of UV radiation and thermal cycling, the diffused moisture induce synergistic degradation of the fiber reinforced polymer matrix composites. For example, Kumar *et al.* [4] have shown that when a carbon fiber reinforced epoxy composite is exposed only to UV radiation, the composite is only affected within 1 to 3 μm from the exposed surface. Nonetheless, in the presence of moisture and UV radiation, the degradation mechanisms lead to continual erosion of the matrix region. Figure 1.4 shows an SEM micrograph of synergistic degradation in an IM7/997 carbon fiber composite.

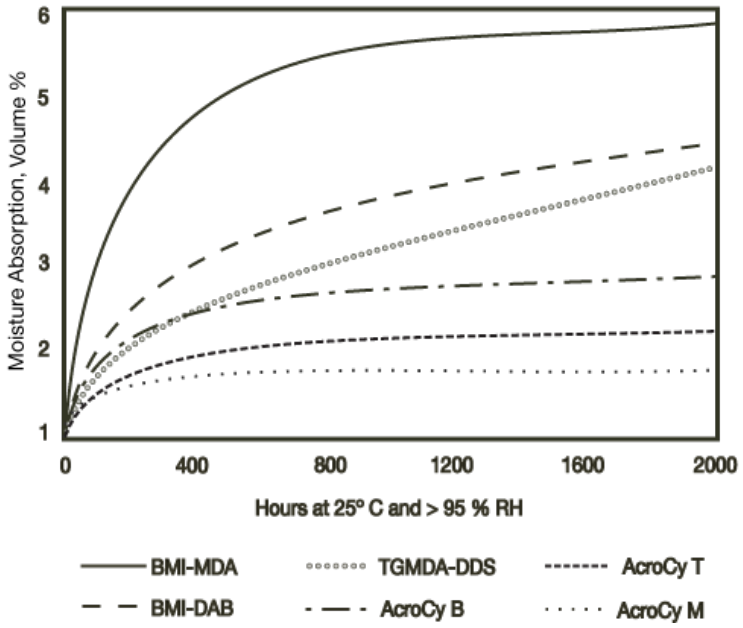

Figure 1.3: Water absorption of 0.125″ thick castings conditioned in a humidity chamber at room temperature for various commercial polymer systems [7].

Boiling Water Degradation

Conventional methods of ageing fiber reinforced polymer matrix composites such as hygric loading, and temperature–humidity ageing have been widely used by several researchers [3, 20–22]. Although these techniques simulate the real life conditions of composite degra-

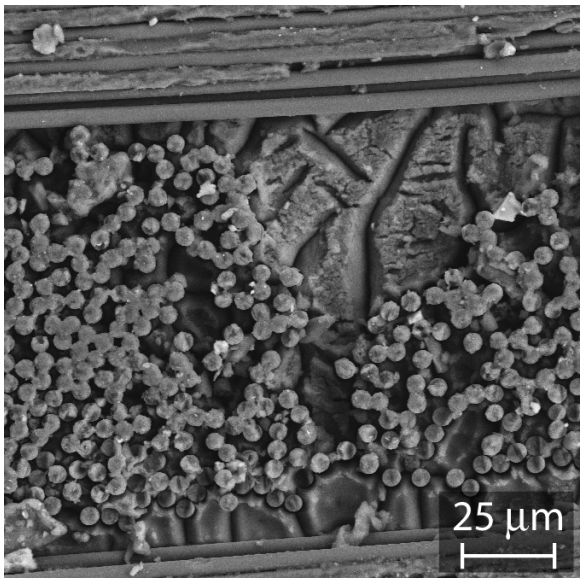

Figure 1.4: Synergistic degradation of an IM7/997 carbon fiber epoxy composite cyclically exposed to UV radiation and water vapour condensation [4].

dation process, they take months if not years to result in any measurable degradation in composite properties. Thus, a more practical way of ageing composite materials is to use accelerated ageing methods like boiling water degradation [19, 23]. Moisture uptake takes place via a diffusion process, the kinetics of which depends on both the relative humidity and temperature. High relative humidities result in a higher moisture absorption rate but it causes a non uniform distribution of moisture within the material domain. However, if the relative humidity is maintained at a constant level while increasing the temperature, the moisture absorption rate increases without causing any non uniformity in the absorbed moisture within the material [19]. Figure 1.5 shows a comparison of the results obtained after Jeevan Kumar *et al.* [24] degraded an IM7/EPON 862 carbon fiber reinforced epoxy composite using temperature humidity ageing and using boiling water degradation. It can be observed from the figure that there is a substantial degradation in the composite properties from the baseline when the composite is degraded using boiling water degradation as opposed to temperature–humidity ageing. Besides, when small microcomposite samples in the form of single fiber composite specimens are aged using boiling water degradation,

the diffusion kinetics speed up substantially. This reduces the period of environmental degradation to a very short amount, further accelerating the ageing process.

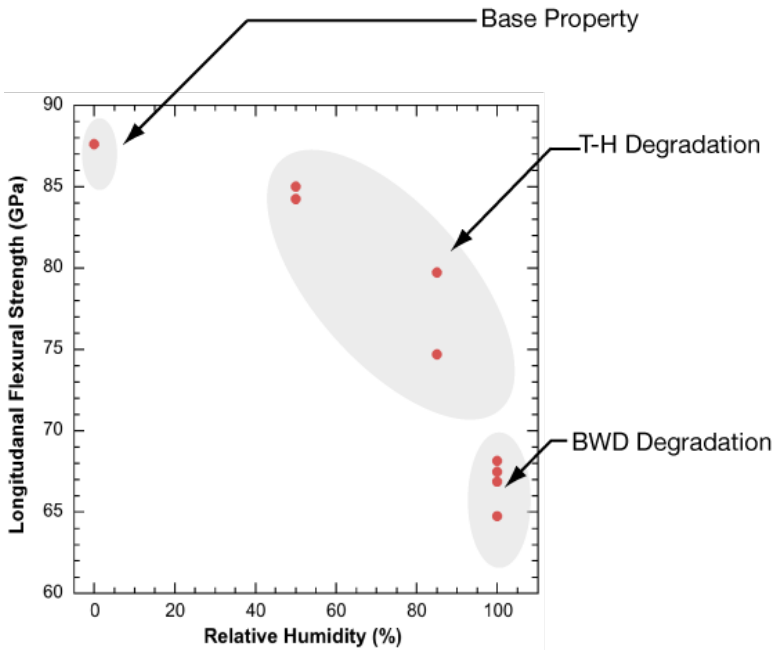

Figure 1.5: Comparison of degradation of IM7/Epon 862 carbon fiber composite using temperature humidity ageing and boiling water degradation [24].

Fluorinated Epoxy Resins

Fluorinated epoxies are polymers produced by reacting one or more fluorinated groups with epoxide groups and can be characterized as thermosets or thermoplastics. Fluorinated epoxies are not much susceptible to the van der Waals forces and hence are highly hydrophobic. Due to these properties, they are widely used for tribological applications. However, they have not yet been used in structural applications like composite materials. A very limited number of researchers have studied fluorinated epoxies as resins for structural materials. For instance, Hayward *et al.* [25] studied the moisture absorption in halogenated resin systems and found that there is a lower percentage of bound water in fluorinated resins. In another instance, Tao *et al.* [26] developed a novel fluorinated epoxy and observed low moisture absorption of the resulting resin formulation. Ding *et*

al. [27] and Wang *et al.* [28] recently conducted similar studies and found similar results. In other studies, Twardowski *et al.* [29], Chong *et al.* [30], and Maity *et al.* [31] studied the wetting and adhesion characteristics of fluorinated epoxies in fiber reinforced composite systems. As can be observed, the moisture absorption and adhesion characteristics have been studied independently for the different fluorinated epoxy composite systems. Furthermore, as explained earlier, the polymer chemists at NASA Langley Research Center have developed novel fluorinated epoxies, and have been studied for their moisture absorption characteristics. Hence, this project aims towards studying the fiber–matrix adhesion of these fluorinated epoxies in fiber reinforced composite systems.

Micromechanical Characterization of the Fiber–Matrix Interface

Any reinforced polymer matrix composite is made up of at least two components, the reinforcements and a matrix. The properties of such a composite material depend not only on the properties of its individual constituents, the fiber and the matrix, but also on the fiber–matrix interface and thus the interphase. On a microscopic level, there is a finite three dimensional region between the bulk fiber and the bulk matrix. This three dimensional region is called the fiber–matrix interphase which has a different structure than the bulk components. The interphase also includes a two dimensional surface called the interface which is the contact region between the fiber and the matrix. Figure 1.6 shows an AFM scan of the cross-section of a fluorinated epoxy carbon fiber microcomposite with the fiber-matrix interface. The interphase region may have a different composition and structure depending on the use of the fiber sizings or treatments employed to enhance the compatibility between the fiber and the matrix [5].

There has been a considerable experimentation done in the area of environmental effects on the structure and properties of fiber reinforced polymer matrix composites. Most of these studies have employed the bulk or macroscopic characterization techniques [3, 20–22].

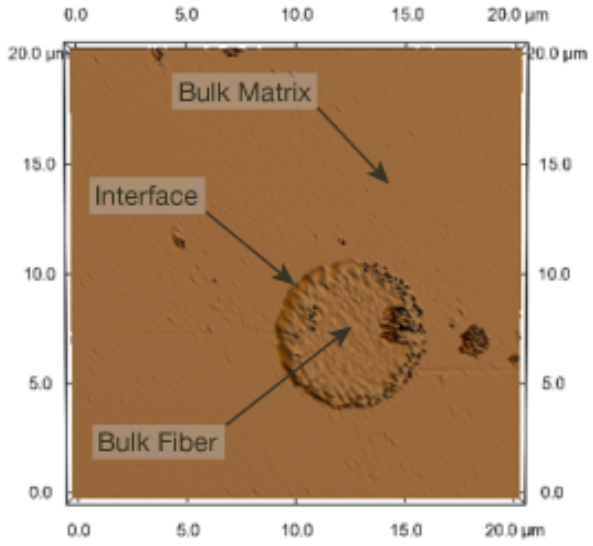

Figure 1.6: AFM scan of the cross–section of a fluorinated epoxy carbon fiber microcomposite showing the fiber–matrix interface.

These tests have a complex process and only provide an overall information about the effects of environment on composite material properties. It is difficult to interpret even the qualitative fiber/matrix properties. However, micromechanical characterization techniques using single fiber composite specimens or microcomposites provide an insight into the fundamental interactions at the fiber-matrix interface and thus serve as a tool for microstructural characterization of composite materials. The amount of adhesion between the fiber and the matrix govern important mechanical properties of a composite in the off axis direction and to some extent along the reinforcement direction.

Several researchers have employed micromechanical techniques to study the interfacial properties of fiber reinforced polymer matrix composites. For example, Andreevska *et al.* [32], Broutman [33], Bartos [35], Bowling *et al.* [34], Mader *et al* [36] and Deng *et al* [37] used the fiber pull–out technique to characterize the interfacial shear strength of the glass polymer systems. Drzal used a single filament fragmentation technique to character-

ize the interfacial failure mode of composite materials in 1980 [38], and similarly followed by Dilandro *et al.* [39], Netravali *et al.* [40], Figueroa *et al.* [42], Curtin *et al.* [43] and many others [5, 41, 44–57] used single fiber fragmentation test for characterizing fiber–matrix interface properties. A few researchers like Wadsworth *et al.* [58] and Mandell *et al.* [59] had used microindentation technique in which they compression loaded the fiber to measure the debond strength of the composite. Miller *et al.* [60] first used the microbond technique to characterize the fiber–matrix interface which was later followed by a large body of investigators such as Gaur *et al.* [61], Biro *et al.* [62], Rao *et al.* [41], Herrerafranco *et al.* [5], Schuller *et al.* [66], Kessler *et al.* [67], Liu *et al.* [68], Nairn *et al.* [69], Pisanova *et al.* [70], and many others [64, 65, 71].

Many researchers have invariably quoted the interfacial shear strength (IFSS) as a measure of fiber-matrix adhesion [72–74]. Besides the ability to probe deep into the microstructure of composite materials, micromechanical tests are also beneficial due to their smaller sizes. These tests only need very minute quantities of materials for fabrication, treatment and analysis. Smaller dimensions ensure rapid degradation kinetics and shorter treatment timescales.

Techniques for Fiber–Matrix Interfacial Strength Characterization

As mentioned above, the fiber matrix interface plays an important role in the performance of fiber reinforced polymer matrix composites since it transfers the stresses from the matrix to the reinforcements and vice versa. Thus, interfacial shear strength is a key measure of the effectiveness of any composite. There are a few experimental techniques that can be used to determine the interfacial shear strength of fiber-reinforced composites at micromechanical level. These include single fiber fragmentation, fiber pull out, micro-indentation, and the microbond test [5, 41]. Figure 1.7 shows schematic illustration of fiber pull out, microindentation and single fiber fragmentation tests.

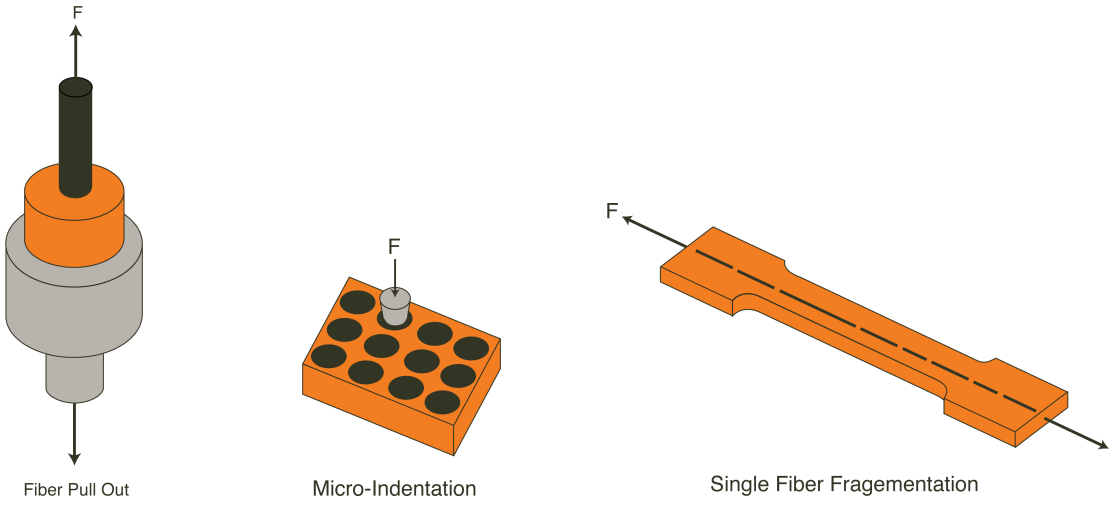

Figure 1.7: Schematic illustration of fiber pull out, microindentation and single fiber fragmentation tests.

Since the fluorinated epoxy of interest is currently being synthesized in very minute quantities, single fiber fragmentation and micro-indentation tests are ruled out as viable fiber-matrix interface characterization techniques. This project employs the micro-bond technique to determine the interfacial shear strengths of fluorinated and non-fluorinated epoxy based carbon fiber reinforced composites and their comparison before and after boiling water degradation. The microbond testing technique involves pulling a single fiber having a microdroplet deposited on it between two knife edged blades of a microvise and recording the force needed to shear the micro-droplet along the length of the fiber, as shown in figure 1.8 [60].

Comparison of Micromechanical and Macromechanical Tests

The greatest skepticism surrounding the validity of micromechanical tests revolves around the relationship between the results obtained by employing micromechanical tests with the conventional bulk scale or macromechanical tests. Several researchers have studied fiber reinforced polymer matrix composites using both, micromechanical and macromechani-

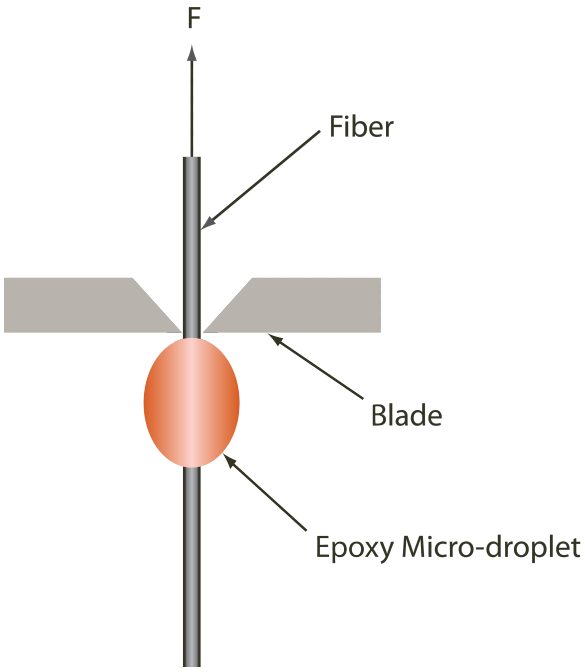

Figure 1.8: Schematic of microbond test

cal characterization techniques. For instance, Herrerafranco *et al.* [75] studied the effects of different types of fiber sizings or surface treatments on carbon fiber epoxy composites using both micromechanical and bulk characterization techniques. They used microbond and microindentation as micromechanical tests whereas Iosipescu and interlaminar shear as macromechanical tests. They observed a change in interfacial shear strength with the changes in fiber surface treatments accompanied with corresponding changes in the shear and interlaminar shear strengths. Mader *et al.* [36] studied composite properties using pull out tests, transverse tension and interlaminar shear. Park *et al.* [76] studied fiber surface treatments on glass fiber polyester resin composites using interlaminar shear, mode II fracture toughness and surface energy variations on fibers. Keusch *et al.* [77, 78] also studied the effect of fiber surface treatments on interfacial shear strength using fiber pull out, interlaminar shear and transverse tension tests. Each of these studies showed that whenever there was any improvement in the macroscopic properties of the composite, there was a corresponding improvement in the micromechanical properties of the composite as well [79]

CHAPTER 2

Materials

The resin used to fabricate microcomposites were supplied by Dr. Jeffrey Hinkley (NASA Langley Research Center, Hampton, VA). They included a fluorinated epoxy and a non-fluorinated epoxy based on tetraglycidyl methylene dianiline (TGMDA). The epoxy resins were deposited on single filament, unsized HexTow IM7 carbon fibers (Hexcel Corporation, Stamford, CA). TGMDA is a tetrafunctional epoxy which is a major component of high performance matrix formulations used for advanced aerospace grade composites. Figure 2.1 shows the chemical structure of tetraglycidyl methylene dianiline epoxy. These epoxies are characterized by high cross-link densities which results in high modulus of elasticity and high glass transition temperature. However, the high crosslink densities of these epoxies are also accompanied with low strain to failure values and high moisture absorption levels [80].

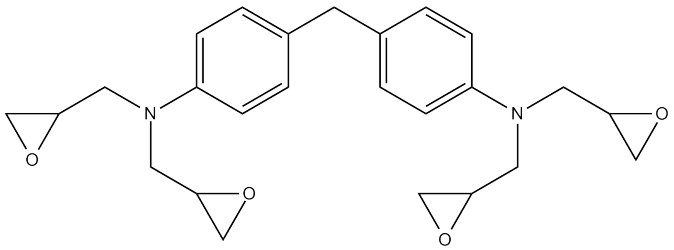

Figure 2.1: Chemical structure of tetraglycidyl methylene dianiline [80].

Diamino diphenyl sulfone (DDS) is the curing agent used with the TGMDA epoxy resin to form the non-fluorinated epoxy used in manufacturing advanced high performance composite materials. DDS when used with TGMDA results in superior thermal stability and mechanical properties such as tensile, flexural and glass transition temperatures [81]. Fig-

ure 2.2 shows the chemical structure of diamino diphenyl sulfone.

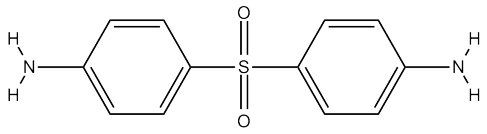

Figure 2.2: Chemical structure of DDS [81].

6F-diamines or 2,2 bis(4-aminophenyl) hexafluoro propane is a fluoropolymer polyimide which when blended with TGMDA forms the fluorinated epoxy studied in this project. Based on the research done at NASA Langley Research Center, these fluorinated epoxies show greatly reduced moisture absorption as compared to the conventional DDS-TGMDA based epoxies [82]. Due to their low moisture uptake characteristics, these fluorinated epoxies could be used as a matrix or as a fiber surface coating in a composite which would therefore potentially result in improved long term durability against environmental effects. However, it remains to be checked if these epoxies have mechanical properties suitable for use in fiber reinforced composites [82].

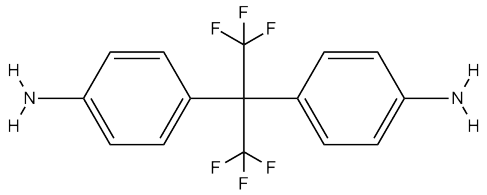

Figure 2.3: Chemical structure of 2,2 bis(4-aminophenyl) hexafluoro propane [82].

The reinforcing fiber used was an as-received HexTow IM7 carbon fiber. HexTow IM7 carbon fiber is a continuous, high performance, intermediate modulus, PAN based fiber available in 12K filament count tows. It has a carbon content of 94.0%, a nominal diameter of 5.2 μm, a tensile strength of 5.57 GPa and a modulus of 276 GPa [83]. Unsized fiber was used in this study to investigate the direct boding of epoxy resins and the carbon fiber surface.

CHAPTER 3

Experimental

Sample Preparation

The microbond procedure involved preparing single fiber specimens by first mounting a single carbon fiber on an aluminum tab. The tab had a 25.4 mm slot where the fiber was suspended as shown in figure 3.1. The fiber was mounted using 'five-minute' epoxy and high temperature aluminum tape. Microdroplets of epoxy were then deposited at the center of gauge length of fiber. This was carried out under an optical microscope at a magnification of 50$\times$ using a special applicator. The applicator consisted of a single carbon fiber mounted on a glass rod. Since both the epoxy resins of interest were semi-solid at room temperature, they were heated in a water bath to make them fluid enough to be picked up and deposited as microdroplets. Furthermore, the applicator was also heated, using a soldering iron, to keep the droplets fluid during deposition. Figure 3.2 shows the arrangement employed to deposit microdroplets of epoxy on single carbon fiber specimens.

A very minute amount of epoxy was then collected on the applicator and applied on the tab mounted carbon fiber samples. When the applicator was retracted, a microdroplet formed and assumed an ellipsoidal shape as discussed by Caroll *et al.* [84]. Typical microdroplets formed had embedded lengths varying from 35 to 50 μm. A batch of 10 microdroplet specimens was made at a time and cured in an oven at 177 °C for 2 hours. It was later realized that this curing schedule was not effective in curing the microcomposites due to the size effects. Since the mass of the epoxy used in fabricating the microcomposites was very low, the heat of reaction which aids in curing, quicky dissipated in the surrounding area. Due to

this dissipation of heat, the microdroplets were not cured completely. The curing schedule was then modified by extending the hold time to 3 hours instead of 2 hours and the epoxy microdroplets were found to have cured completely.

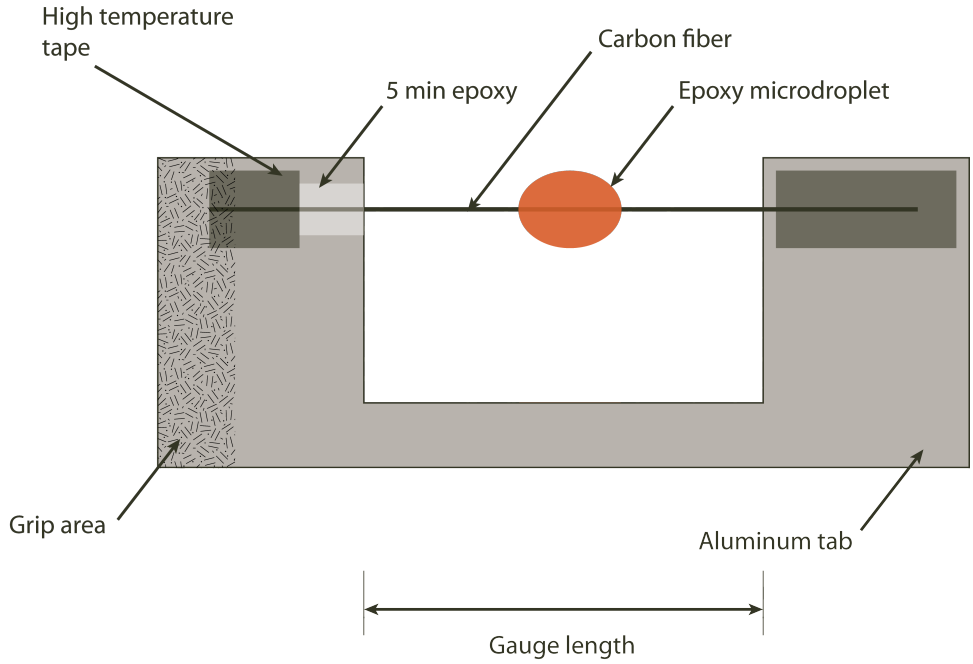

Figure 3.1: Schematic illustration of mounting tab used for fabricating microcomposite specimens.

Both, the fiber diameter and the microdroplet dimensions were required for analysis of microbond tests. The diameter of the fibers were measured using Fraunhofer slit diffraction principle with a Helium-Neon laser as shown in figure 3.4. The microdroplet dimensions, namely the major axis or the embedded length and the minor axis were measured under a Nikon Eclipse L150 optical microscope using a traveling stage. Figure 3.3 shows an optical image of a microdroplet on a single carbon fiber.

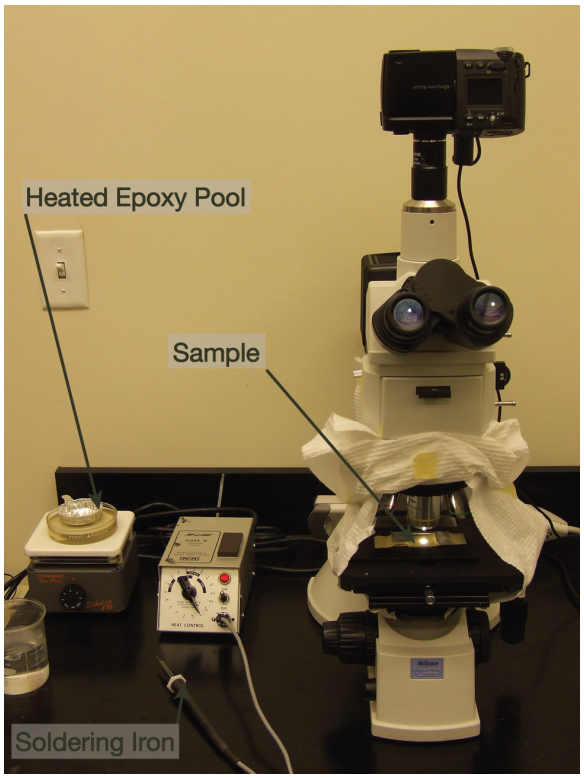

Figure 3.2: Setup for depositing epoxy microdroplets on single fiber specimens.

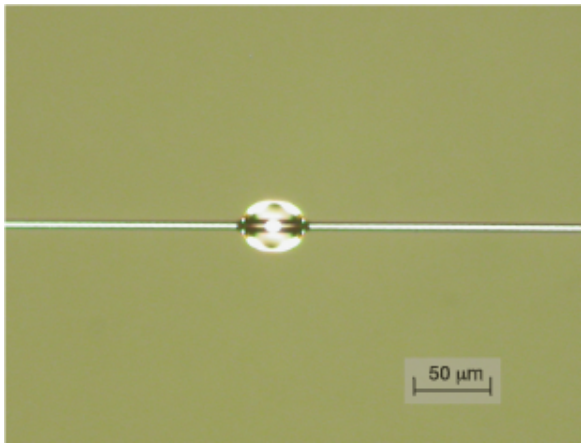

Figure 3.3: Optical image of a microdroplet deposited on a carbon fiber at 50x magnification

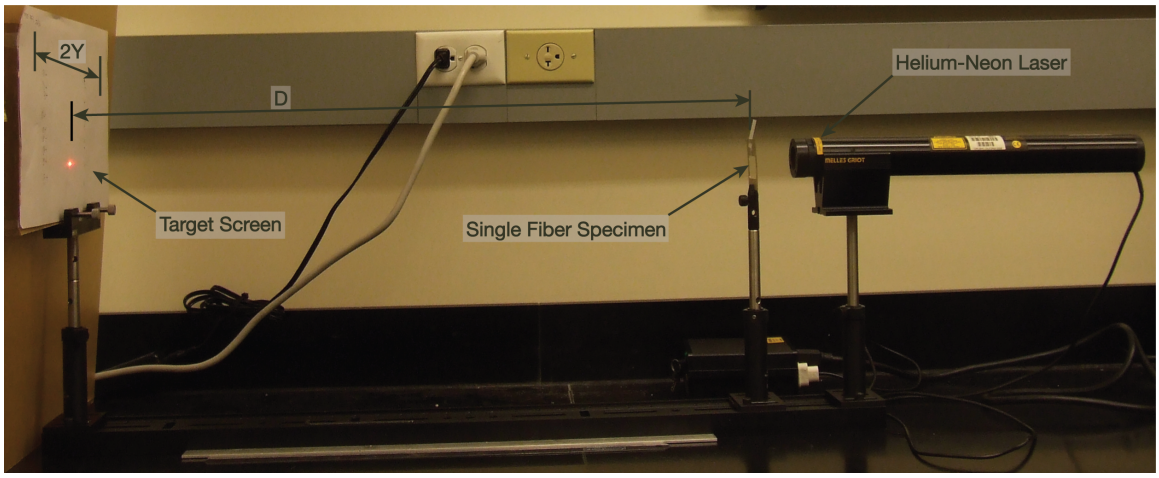

Figure 3.4: Fiber diameter measurement using Fraunhofer slit diffraction setup

Microbond Tests

The microcomposite specimens were loaded using a microvise on an Instron 5567 tensile testing machine equipped with a 10 N load cell to determine the debond force. The microvise consisted of Aluminum forks mounted on an Aluminum base. Two knife-edged blades were fastened on top of the forks. A micrometer screw with a least count of 0.5 μm was mounted on the top of the fork to adjust the gap between the blades. Figure 3.5 shows a schematic illustration of the microvise loading fixture. The top end of the aluminum tab was clamped and suspended on the load cell which was further connected to the crosshead whereas the lower end of the aluminum tab was passed through the opening between knife edged blades of the microvise which was fixed to the stationary platen of Instron. The crosshead was then adjusted such that the microdroplet was located just below the blades. The gap between the microvise blades was then reduced by adjusting the micrometer screw attached to the fork of microvise. Contact was identified when there was a slight increase in the force recorded by load cell while the crosshead was being moved. Figure 3.6 shows a specimen ready for testing.

The crosshead and thus the fiber were then pulled between the microvise blades at a rate

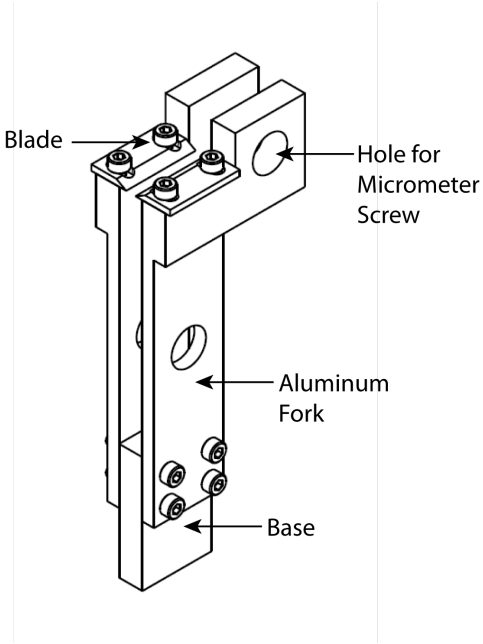

Figure 3.5: Schematic illustration of microvise loading fixture

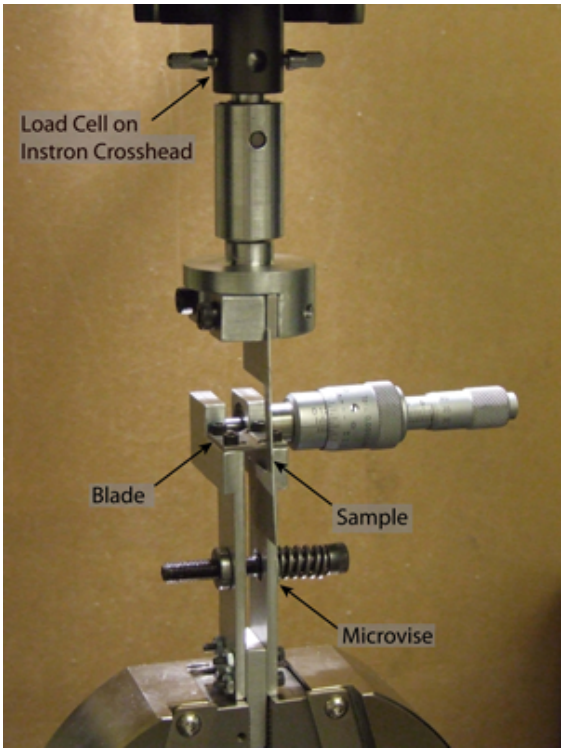

Figure 3.6: Microbond experimental setup

of 1 mm/min. As the fiber was being pulled, the microdroplet moved with the fiber and at a certain point, established contact with the lower surface of the microvise blades. After this contact, the load from the fiber was transferred to the fiber–matrix interface under shear. In a typical experiment, the load reached a peak value and then dropped suddenly to a very low value. The post-shear failure load was slightly greater than the initial force due to the frictional force between the sliding microdroplet and the fiber. The peak force was identified as the force when the interfacial stress reaches its maximum value and hence represented the interfacial shear strength.

Using a simple analysis, that assumes a uniformly distributed state of pure shear, the interfacial shear strength of the microcomposite can be determined as given by equation 3.1.

$$\tau_{int} = F_d/\pi D_f l_e \tag{3.1}$$

Where F_d is the pull out force, D_f is the fiber diameter, l_e is the embedded length, and τ_{int} is the interfacial shear strength. Note that if the embedded length of the fiber had been greater than the critical fiber length, this loading would have resulted in a fiber tensile failure. The microcomposite specimens that were tested after ageing were degraded using boiling water degradation for 24 and 48 hours. The procedure consisted of mounting the specimens on an aluminum holder and putting it inside a beaker filled with 1000 ml distilled water. The beaker was suspended in a silicon oil bath to ensure uniform heating and had a condenser mounted on the top to avoid evaporation of water. The entire setup was placed on a heating plate, which was heated to a temperature of 295 °C. This ensured continuous boiling of water and subjected the specimens to a condition of 100 °C at 100% relative humidity. Figure 3.7 shows the boiling water setup used to degrade the microcomposites.

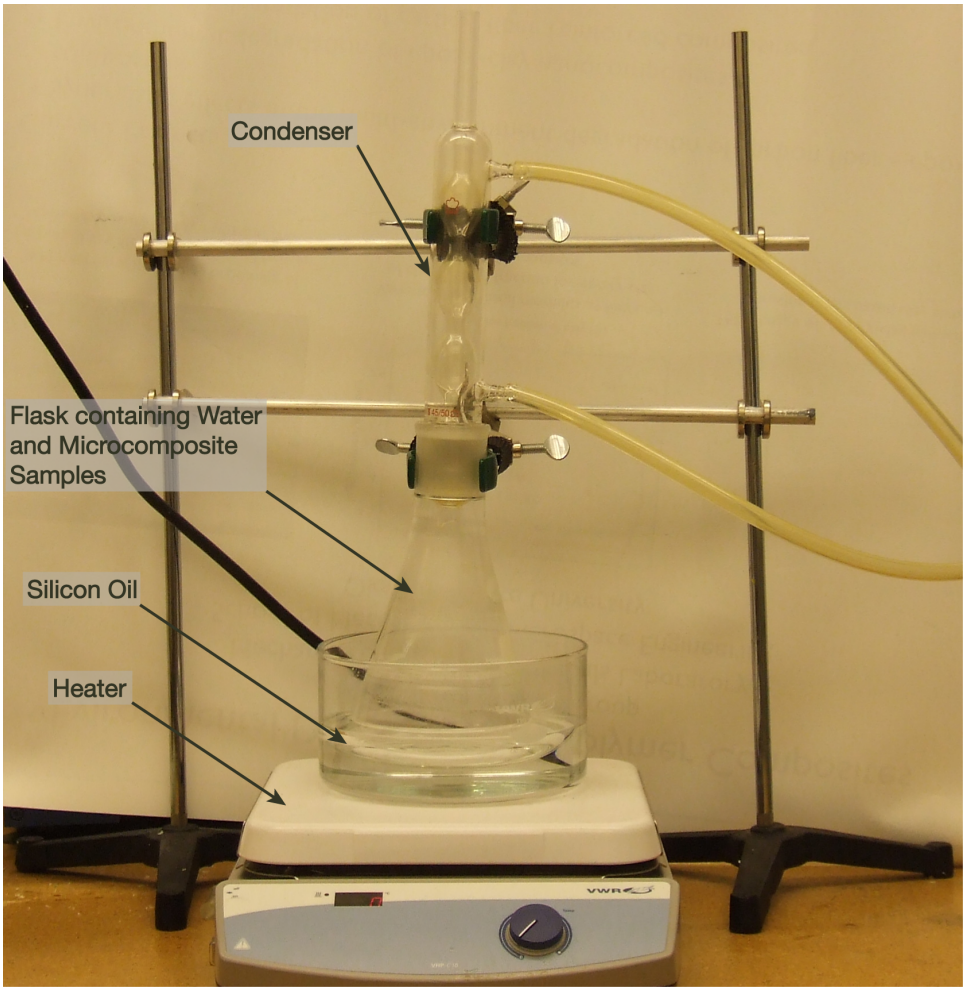

Figure 3.7: Accelerated ageing of microcomposites using boiling water degradation

Finite Element Modeling

The most commonly adopted method for evaluating stresses in the microbond test is the finite element method [5, 65–67, 85, 86]. The simple shear analysis used to determine the fiber-matrix interfacial shear strength assumes that the shear stress is uniformly distributed along the embedded length of the fiber. However, In practice, the shear stress varies along the embedded length. The shear analysis also assumes that the loading results in a pure debonding type of failure. However, due to the meniscus formation, a very small length of the microdroplet up to the point of contact of the blades is fractured and remains fixed along the fiber followed by debonding of the remaining length of microdroplet. This introduces

a large scatter in experimental results. Thus, in this study the microbond test was modeled using finite element analysis to determine the variation of interfacial shear strength along the embedded length of the fiber. ABAQUS CAE 6.7.4 from Dassault Systemes was used for this purpose.

The first step in modeling the finite elements microbond test was construction of the microdroplet shape. Some authors have reported that the geometry of the micro-droplet does not play a significant role in the resulting interfacial stresses [65]. The analysis of circular, spherical, and elliptical shape microdroplets have been commonly reported in the literature. When a microdroplet is deposited on a fiber, the liquid droplet ends form a meniscus due to the capillary forces, where the formed shape remains upon polymer curing. Neither circular nor elliptical shape results in a meniscus. The geometry for the finite element model was thus modeled using a combination of elliptical section and fillet radii at the ends. The dimensions used were taken from an experiment conducted on epoxy EPON 862/Epikure 3234 microdroplet on an as-received IM7 carbon fiber. The dimensions used were an embedded length of 78.89 μm, a microdroplet minor axis of 56.27 μm, and a fiber radius 3.5 μm. Figure 3.8(a) shows the microbond test assembly.

In order to simplify the model no interphase region was introduced. Dimensions of the blade were taken from the actual dimensions of the blade used in the experiment. The microvise blade was modeled with a fillet radii of 5 μm and a fiber-blade gap of 5 μm. The fiber and the microdroplet were modeled as two-dimensional deformable axisymmetric parts and the blade was considered to be two-dimensional axisymmetric rigid part. A very fine mesh was required where the blade contacts the microdroplet, and the mesh was biased accordingly. This contact between the blade and microdroplet was modeled using contact interaction without friction. Element size of 0.2 μm was used in the region of contact and 0.6 μm was used elsewhere. 3 and 4-node bilinear axisymmetric elements were

used to mesh the microdroplet. Figure 3.8(b) shows the results after meshing the microdroplet. Finally, a geometrically nonlinear stress analysis was carried out to evaluate the stress variation at the interface. The boundary conditions imposed on the model were a vertical roller support at the left edge of the fiber, horizontal roller support at the top end of the fiber, and the left edge of the fiber as the axis of symmetry. A downward load of 100 mN was applied on the blade after making firm contact between blade and the microdroplet. Blade was encastered to result in zero degree of freedom. Figure 3.8(c) shows the results of the microbond model after imposing the boundary conditions and contact interactions. The load was the actual load needed to debond the microdroplet from the fiber in the microbond experiment carried out on the specimen of which the dimensions were used above. The material properties used for modeling the epoxy microdroplet were obtained from the EPON 862/EPIKURE 3234 data sheets from Hexion Specialty Chemicals Inc, Columbus, OH [87]: Youngs modulus of matrix as 3.3 GPa, Poissons ratio as 0.35, Youngs modulus of fiber as 270 GPa, and Poissons ratio as 0.25. The matrix was also modeled as an elastic perfectly plastic material with a yield stress of 106 MPa to compare with the elastic solution.

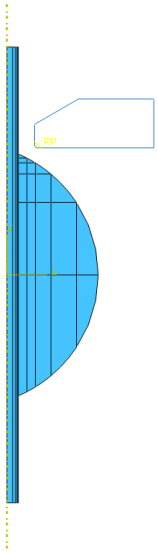

(a) Finite element model of the microbond test

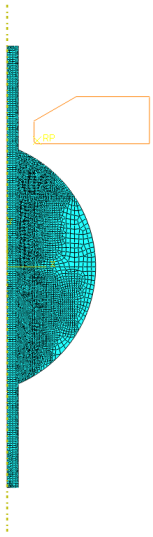

(b) Finite element mesh of microdroplet using biased 3 and 4 node bilinear axisymmetric elements

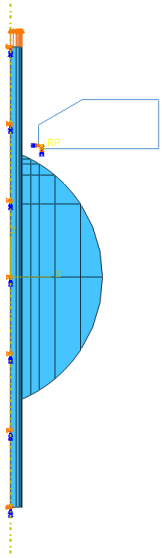

(c) Contact interactions and boundary conditions on the finite element microbond model

Figure 3.8: Finite element modeling of microbond test.

CHAPTER 4

Results and Discussion

Failure Mode, Valid and Invalid

Figure 4.1 shows a typical load displacement curve of a microbond experiment after a successful fiber–matrix interface failure. As the fiber moved upward with the crosshead, the microdroplet made contact with the microvise blades and thus the tensile force on the fiber was transferred to the fiber–matrix interface which was recorded by the load cell. The load then increased linearly until a peak force F_d was reached. At this point the interfacial bond

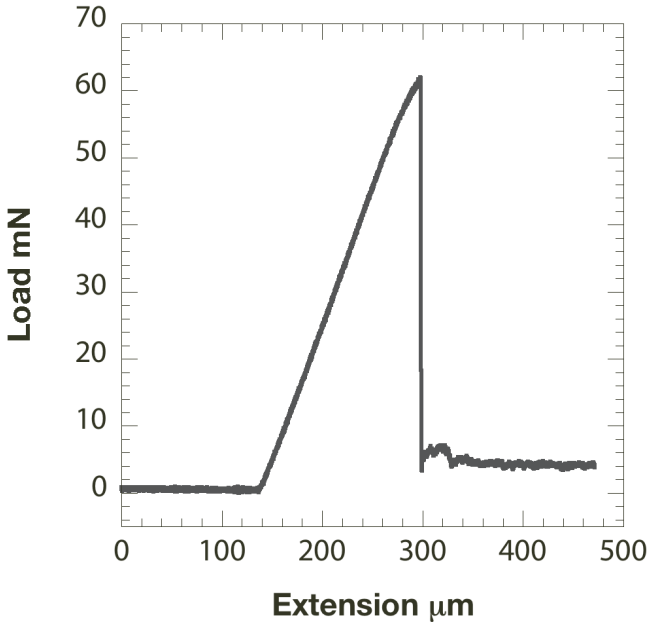

Figure 4.1: Typical microbond load displacement curve.

strength of the microcomposite was reached and the interface failed followed by sliding of the microdroplet on the fiber with a frictional force F_f. Figures 4.2(a) and 4.2(b) show SEM micrographs of a degraded IM7 carbon fiber/6F–TGMDA epoxy microcomposite be-

fore and after fiber–matrix failure respectively.

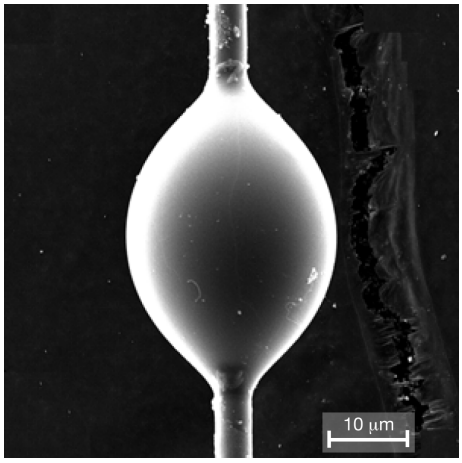

(a) SEM micrograph of an IM7 carbon Fiber/ 6F–TGMDA epoxy microcomposite degraded for 48 hours using boiling water degradation before fiber–matrix interfacial failure.

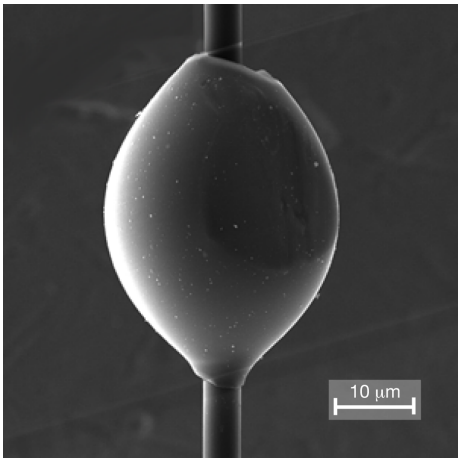

(b) SEM micrograph of an IM7 carbon fiber/ 6F–TGMDA epoxy microcomposite degraded for 48 hours using boiling water degradation after fiber–matrix interfacial failure.

Figure 4.2: SEM micrographs of microcomposite before and after interfacial failure.

However, the probability of obtaining successful fiber–matrix interface failure from a microbond experiment is low since many experiments result in unwanted failure modes like fiber tensile failure, cohesive failure of microdroplet, or handling failures as shown in figure 4.4. Excluding the initial experiments done on a different epoxy system, it was observed that only about 17% tests resulted in fiber–matrix interfacial failure while 54% were fiber tensile failures, about 21% cohesive failures, and the remaining 8% resulted in fiber failure either during handling or clamping the sample between the microvise blades. For instance, when the interfacial shear strength of a microcomposite exceeded the ultimate fiber tensile strength, the microbond experiment resulted in a fiber tensile failure as shown in figure 4.5(a). Such tensile failures occured consistently near the region just above the embedded length of the fiber. Besides observing the microcomposite under an optical microscope, fiber tensile failure can also be identified from the load displacement trace. For

instance, the load overshoots below the initial level immediately following a fiber tensile failure event, as shown in figure 4.3(a). This is perhaps due to stress concentration near the end of the microdroplet.

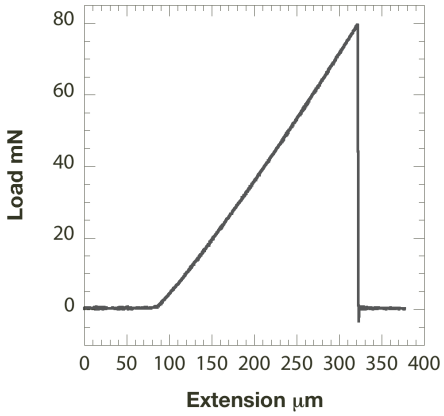

(a) Load displacement trace obtained during a fiber tensile failure of an IM7 carbon fiber/ DDS–TGMDA microcomposite in a microbond experiment.

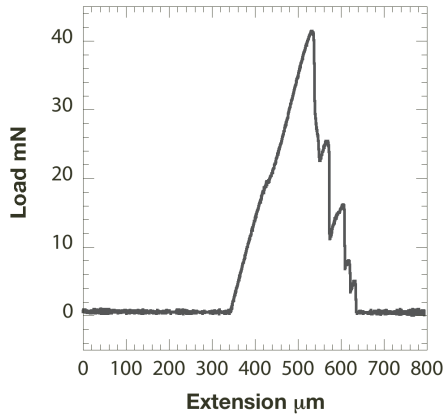

(b) Load displacement trace obtained after a cohesive failure of a microcodroplet in an IM7 carbon fiber/ DDS–TGMDA microcomposite.

Figure 4.3: Load displacement trace during invalid failure modes

In another instance. when the gap between the microvise blades and the fiber was greater, and the microdroplet dimensions were greater, it resulted in a cohesive mode of failure of epoxy microdroplet as shown in figure 4.5(b). This was also identified in the load trace by its characteristic load fluctuation following the cohesive failure event as shown in figure 4.3(b). Results from failure modes other than interfacial were not included for interfacial shear strength calculations. Futhermore, depending on fiber–blade gap, and the embedded length of fiber–matrix interface, a small amount of resin remained adhered to the fiber after the interfacial debonding of the microdroplet. This adhered region is called the meniscus and was corrected for during the calculations of interfacial shear strength. The meniscus effect was not observed in microcomposites that were aged using boiling water

degradation. Figures 4.6(a) and 4.6(b) show the interfacial failure with and without the adhered meniscus.

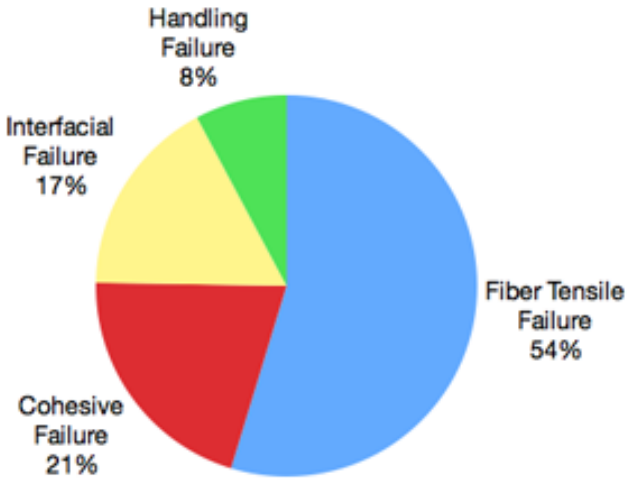

Figure 4.4: Proportion of various failure modes during a microbond experiment.

Interfacial Shear Strength

Several batches of microcomposite specimens were tested over a period of time with each batch consisting of at least ten samples. As discussed earlier, the interfacial shear strength of microcomposites was determined. The interfacial shear failure of fiber reinforced polymer composites is dependent on the statistical flaw distribution along the embedded length of the fiber within the microdroplet. Furthermore, the random variable representing the interfacial shear strength will always assume positive values and thus it is an asymmetrical function about the mean. These characteristics rule out the use of normal distribution and other similar functions and hence, Weibull analysis was carried out on the resulting groups of data in accordance with the ASTM C 1239–07. The Weibull probability distribution

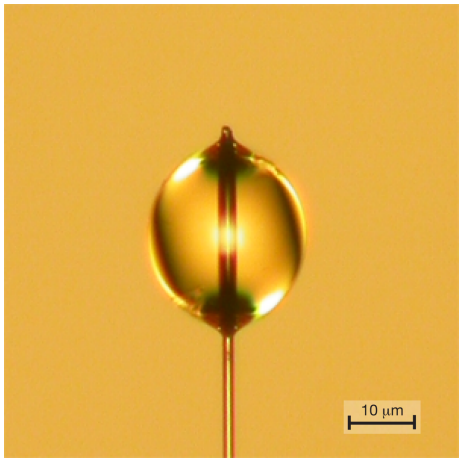

(a) Optical image of an IM7 carbon fiber/ DDS–TGMDA microcomposite at 50X after fiber tensile failure in a microbond experiment.

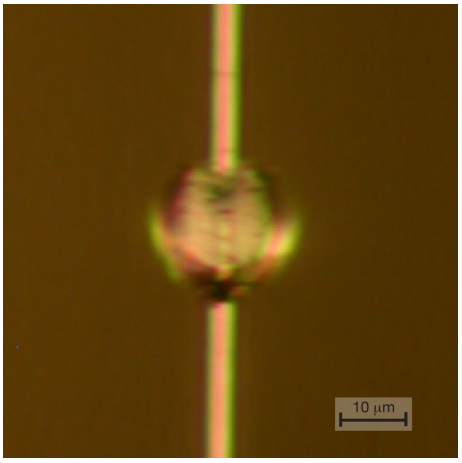

(b) Optical image of an IM7 carbon fiber/ DDS–TGMDA microcomposite at 50X after cohesive failure of epoxy microdroplet.

Figure 4.5: Optical micrographs of microcomposites after invalid failure modes

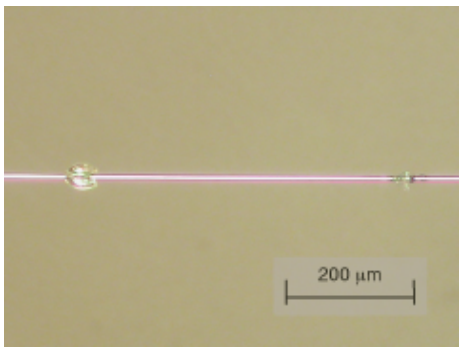

(a) Interfacial failure before boiling water degradation – meniscus present

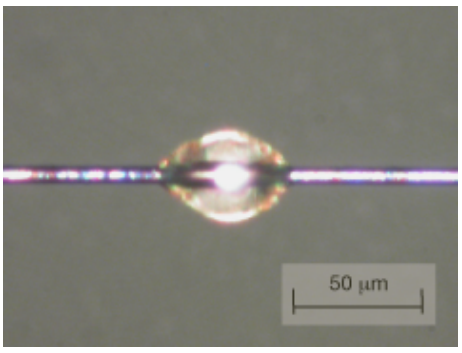

(b) Interfacial failure after boiling water degradation – meniscus absent

Figure 4.6: Fiber–matrix interface failure with and without meniscus effect.

function is given by:

$$P_f = 1 - \exp[-(\sigma/\sigma_\theta)^m]\sigma > 0 \tag{4.1}$$

Where P_f is the probability of failure, σ_θ is the Weibull characteristic strength and m is the Weibull modulus.

Weibull probability plot for interfacial shear strengths of fluorinated, non–fluorinated, before and after ageing using boiling water degradation is shown in figure 4.7. It was observed that the Weibull modulus for both, fluorinated epoxy microcomposite and non–fluorinated epoxy microcomposite, was identical before boiling water degradation. Similary, the Weibull modulus was identical for the two systems after being aged using boiling water degradation. However, the Weibull modulus for the microcomposites aged using boiling water degradation increased subsequent to ageing. The idential Weibull moduli for the two epoxy systems indicated similar variability and defects in chemical bonding between the fiber and the epoxies. Increased but identical Weibull moduli of aged microcomposites indicated that the variation in adhesion after ageing remained similar in the two epoxy systems but at the same time, variation in adhesion decreased due to possible breaking of the remaining chemical bonds between the fiber and the matrix.

The results obtained after Weibull analysis of interfacial shear strength data of the two microcomposite systems are summarized in Table 4.1. As can be seen, the interfacial shear strength of the fluorinated epoxy based carbon fiber composites was higher than that of the non–fluorinated epoxy based carbon fiber composites when the microcomposites had not been not aged. Both the micrcomposite systems underwent a reduction in interfacial shear strength after being aged using boiling water degradation. There was a significant, about 43% reduction in interfacial shear strength of fluorinated epoxy based microcomposites as

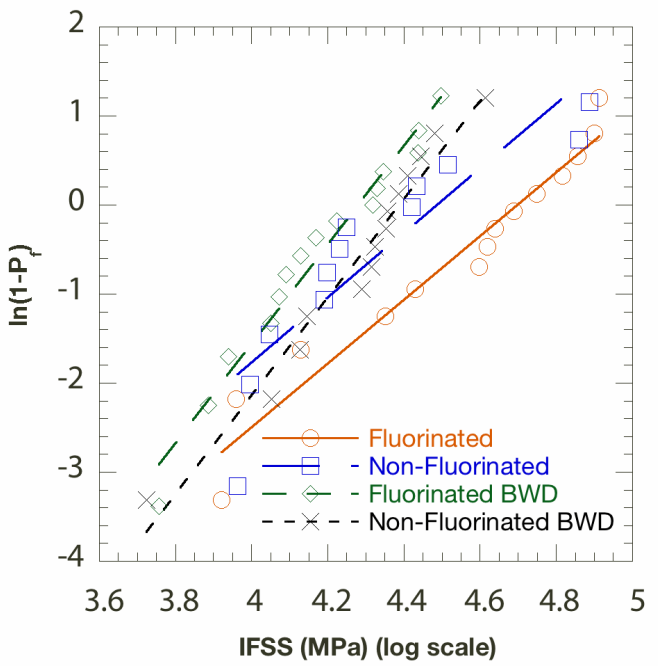

Figure 4.7: Weibull probability plots for comparison of interfacial shear strengths of different epoxy microcomposite systems and degradation conditions.

opposed to only 9.2% decrease in the interfacial shear strength of non–fluorinated epoxy based microcomposites. This indicated that the fluorinated epoxy based microcomposites underwent relatively higher levels of degradation than their non–fluorinated epoxy counterparts.

Fiber	Matrix	Degradation	IFSS (MPa)	Weibull Modulus
IM7	DDS-TGMDA	None (As received)	88.7	3.2
IM7	6F-TGMDA	None (As received)	94.8	3.2
IM7	DDS-TGMDA	BWD for 48h	80.5	5.5
IM7	6F-TGMDA	BWD for 48h	53.5	5.0

Table 4.1: Experimental results for fluorinated and non–fluorinated epoxy carbon fiber composite systems before and after boiling water degradation

The adhesion between the fiber–matrix interface in the microcomposites is characterized by weak dispersion forces (van der Waals forces) between the functional groups on surface of the fiber and on the matrix, and strong local bonds (chemical bonds) between the fiber and the matrix molecules. When the microcomposites were subjected to boiling water degradation, the adhesive bonding between the fiber and the matrix was weakened. Water molecules diffused into the interface via flaws in the fiber, the matrix or the fiber–matrix interface. The diffused water molecules might have damaged the chemical bonding at the interface causing a permanent irreversible damage due to hydrolysis. Intuitively, one would hypothesize that since the fluorinated epoxy underwent reduced moisture absorption, it would exhibit reduced plasticization at the matrix and reduced hydrolysis at the fiber–matrix interface. However, the results indicated otherwise. Perhaps, even though the fluorinated epoxy microcomposite experienced reduced moisture diffusion through the microdroplet, it failed to resist the diffusion of water up to the fiber–matrix interface via capillary action at the meniscus region. The diffused water molecules at the fiber–matrix interface disrupted the intermolecular hydrogen bonding resulting in substantially reduced interfacial shear strength. The relative difference of degradation in interfacial shear strength between the two epoxy microcomposite systems could be explained by chemical bond analysis at the interface. In order to explain this counter intuitive observation, Raman spectroscopy was attempted to analyze the two microcomposite systems, however, it resulted in a very low signal to noise ratio and damaged the microcomposite systems at higher gains. It was also postulated that these differences could be due to the difference in residual stresses which can be detected by post debonding friction.

Interfacial Friction

Interfacial shear strength can also be influenced due to the residual stresses developed due to thermal shrinkage difference between the carbon fibers and the epoxy matrix. In order to understand this effect of residual stresses on the interfacial shear strength, an approximate

Fiber	Matrix	Degradation	Friction Stress (MPa)	Weibull Modulus
IM7	DDS-TGMDA	None (As received)	4.5	0.8
IM7	6F-TGMDA	None (As received)	7.5	1.7
IM7	DDS-TGMDA	BWD for 48h	6.2	1.8
IM7	6F-TGMDA	BWD for 48h	9.1	2.3

Table 4.2: Friction stress results for fluorinated and non–fluorinated epoxy carbon fiber composite systems before and after boiling water degradation

analysis of the post–debonding microdroplet friction was performed. After the fiber–matrix interface failure, the microdroplet slides along the fiber with a force F_f which was measured by the load cell. The friction stress was then determined by:

$$\tau_f = F_f/\pi D l_e \tag{4.2}$$

Where F_d is the frictional force at the fiber–matrix interface after interfacial failure, D is the fiber diameter, and l_e is the embedded length of the fiber–matrix interface. Friction stress was calculated for both, the fluorinated epoxy based microcomposites and the non–fluorinated epoxy based microcomposites before and after being aged using boiling water degradation. Further, Weibull analysis was performed on the friction stress data. Figure 4.8 shows a comparison of friction stress between the two epoxy microcomposite systems before and after boiling water degradation. It was observed that the Weibull modulus was greater for the fluorinated epoxy microcomposite after boiling water degradation relative to the other microcomposite systems. This suggested that there was a greater variation in the adhesional pressure between the fiber and the matrix in the non–fluorinated epoxy before being aged relative to the other remaining microcomposite systems. Table 4.2 shows results of the Weibull analysis on friction stress data. It was observed that the friction stress increased substantially after the microcomposites were aged using boiling water degradation. For instance, there was an increase of 21% in friction stress in fluorinated epoxy

based microcomposites and an increase of 28% in the non–fluorinated epoxy based microcomposites. Since the curing conditions for the two epoxies were same, the greater increase in friction stress in non–fluorinated epoxy microcomposites suggested that the non–fluorinated epoxy underwent higher swelling due to boiling water degradation and hence experienced a greater post–debond friction. It was also observed, that on an average, the friction stress was within about 10% of the interfacial shear strength values. Thus, the effect of residual stresses on the interfacial shear strength were ignored.

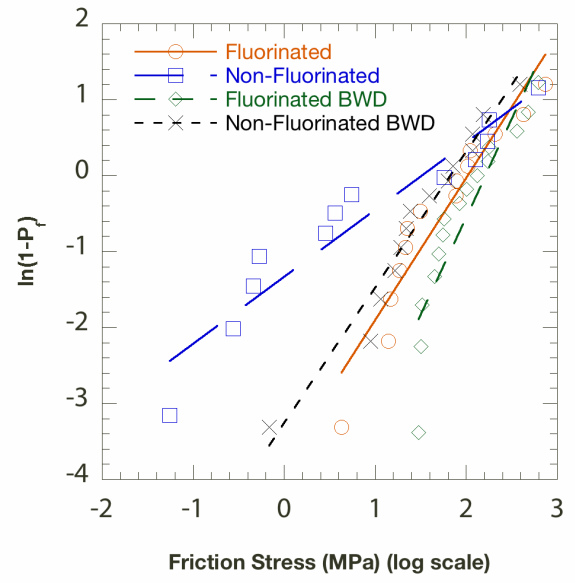

Figure 4.8: Weibull probability plots for comparison of friction stress of different epoxy microcomposite systems and degradation conditions.

Influence of Microdroplet Geometry

The influence of microdroplet geometry on the interfacial shear strength of microcomposites was studied by analysing the variation of interfacial shear strength with fiber–matrix embedded length, fiber–matrix interfacial area and the microdrolet volume as shown in figures 4.9, 4.10 and 4.11. It was observed that the interfacial shear strength increased as the embedded length of the fiber was decreased. Further, it was also observed that the distribution of interfacial shear strength decreased with increasing fiber–matrix contact or

increasing microdroplet volume. This observed influence of the microdroplet dimensions on the interfacial shear strength of the microcomposites was due to the fact that the simple strength of materials based approach of determination of interfacial shear strength is very simplistic and global. This approach also was responsible for the observed scatter in the experimental data, thus making it difficult to obtain reproducible results amongst different researchers. Recently, Pisanova *et al.* have determined that by defining a local parameter for interfacial shear strength in terms of the ultimate interfacial shear strength, the results obtained are much more accurate, reproducible and comparable [70].

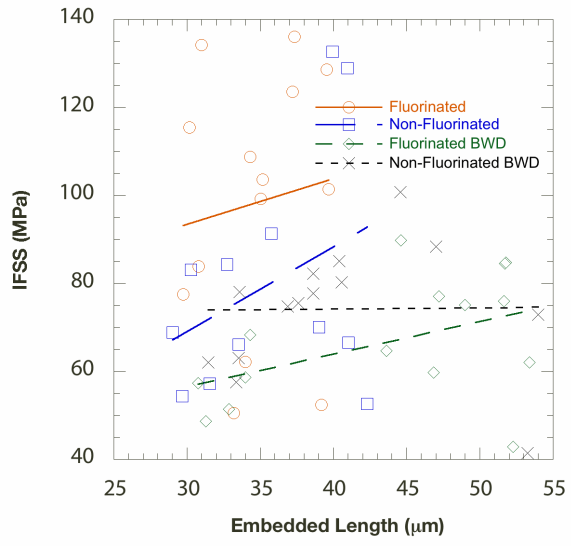

Figure 4.9: Effect of embedded length on interfacial shear strength.

Finite Element Results

The stress distribution along the interface of fiber and microdroplet in a microbond test was calculated by using finite element analysis. The results were compared by plotting the normalized stresses versus the normalized length along the fiber–matrix interface. The error in average shear stress along the interface calculated from the FEM and the experimental IFSS was approximately 5%. The contour plots of shear stress for the elastic and elastic–perfecty–plastic microbond models are shown in figures 4.12(a) and 4.12(b). As can be

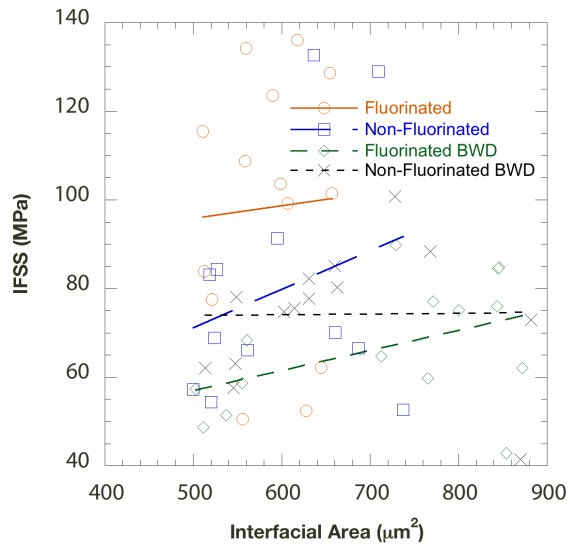

Figure 4.10: Effect of interfacial area on interfacial shear strength.

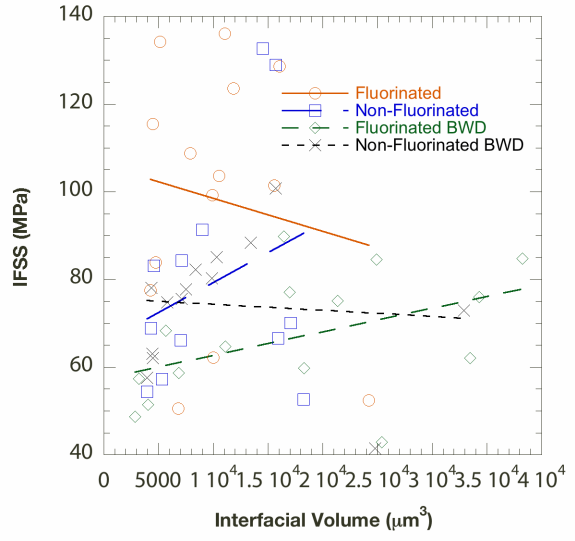

Figure 4.11: Effect of microdroplet volume on interfacial shear strength.

observed in the elastic model the contour of maximum shear stress started from the point of contact between blade and the microdroplet and it extended up to the interface. Along the interface the shear stress was maximum in the vicinity of the blade–microdroplet contact point. The shear stress reduced on moving away from the blade. Whereas, in the elastic–perfectly plastic model the shear stress was constant along the interface except around the blade–microdroplet contact point. The elastic–perfectly–plastic model of microbond represents the condition of microcomposites when the epoxy crosslink densities are not high. As explained earlier, the strength of materials based approach of determination of interfacial shear strength is too global since the interfacial shear strength varies substantially along the embedded length. Figure 4.13 shows a normalized plot of interfacial shear strength along the normalized distance on fiber–matrix interface. As can be observed, the normalized shear stress was maximum near the region where the fiber–matrix embedded length began and reduced down further along the embedded length.

It has been recently shown that a more accurate parameter to characterize the fiber–matrix interfacial bond strength is the ultimate interfacial shear strength τ_{ult} [70]. Equations exist for the calculation of the ultimate interfacial shear strength, however, it also needs mechanical and physical properties of the matrix other than the debond force values and fiber properties. Since the epoxies synthesized by NASA were available in very minute quantities, characterizing the physical and mechanical properties of the epoxies was not feasible and thus it ruled out calculating the ultimate interfacial shear strength. However, It was decided to pursue mechanical and chemical characterization studies of the epoxy systems as the future work which is discussed in the next section.

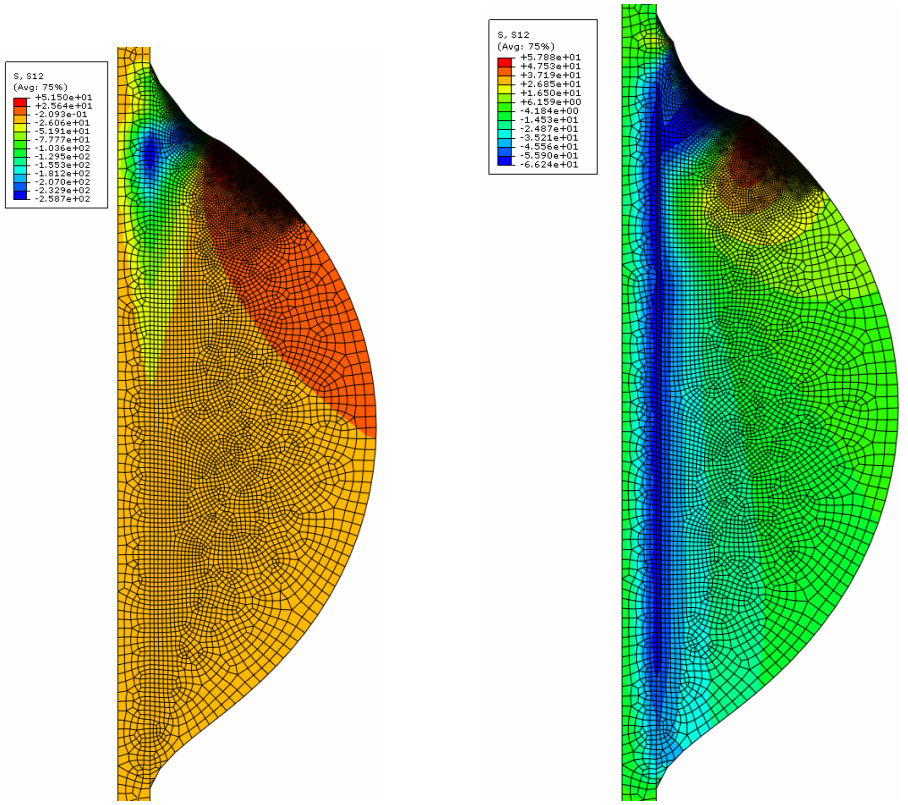

(a) Contour plot of shear stress for elastic model of microbond test

(b) Contour plot of shear stress for elastic–perfectly–plastic model of microbond test

Figure 4.12: Finite element results of microbond test.

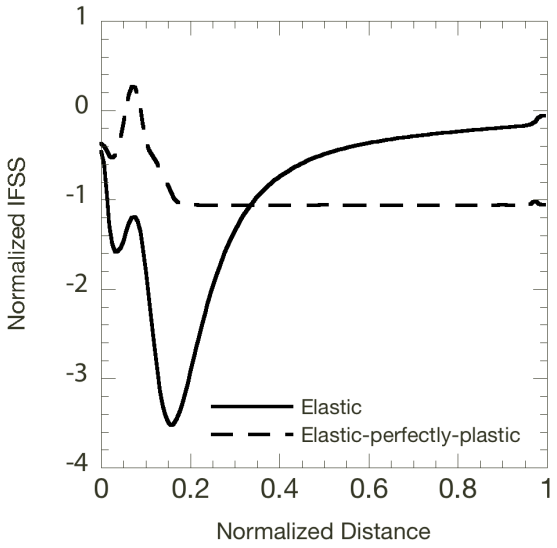

Figure 4.13: Normalized shear stress along the normalized fiber distance.

CHAPTER 5

Conclusions and Future Work

It is clear from the results obtained from this project that before any novel epoxy or sizings are established for a fiber reinforced polymer matrix composite, the adhesion between the fiber and the resin system must be evaluated for optimum performance of the composite system. A novel fluorinated epoxy was synthesized which exhibited reduced moisture absorption but its adhesion properties were not known. The microbond technique was used to study the interfacial shear strength of this novel fluorinated epoxy as well as the conventional non-fluorinated epoxy based single carbon fiber composites. The single fiber composites fabricated based on the two epoxy systems were aged using accelerated degradation technique in the form of boiling water degradation. The failure modes of the microcomposite specimens were tracked during the microbond testing. There was a low probability of obtaining successful fiber-matrix debonding failure mode occuring due to the accompanying failure modes like fiber tensile failure and cohesive failure modes.

The experimental results show that the interfacial shear strength of fluorinated epoxy based single fiber composites was higher than its non-fluorinated counterpart. There was a significant reduction in the interfacial shear strength after the microcomposite systems were aged for 48 hours using boiling water degradation. The interfacial shear strength of fluorinated epoxy based microcomposites was decreased by 43% after ageing whereas there was a 9.2% decrease in the interfacial shear strength of non-fluorinated epoxy based microcomposites after ageing.

The effect of interfacial frictional stress on the interfacial shear strength was studied by performing post debonding friction analysis. It was found that the friction stresses were within 10% of the interfacial shear strength of the microcomposites ruling out any requirements to conduct residual stress analysis. The effect of meniscus was taken into account for calculating the interfacial shear strengths of microcomposites that were not aged. The influence of microdroplet geometry on the interfacial shear strength of microcomposites was studied and it was observed that a decrease in embedded length of microcomposite increased the interfacial shear strength. Finite element modeling of the microbond test was done to evaluate the variation of the interfacial shear stress along the embedded length of the microcomposite. It was confirmed that the interfacial shear stress was highest at the region near fiber entry and near the region where the blade made contact with the epoxy microdroplet. It was confirmed that the average interfacial shear strength parameter was not a very accurate metric for qualifying the performance of a fiber/matrix system in a fiber reinforced polymer matrix composite.

There are a few things which can be addressed to further understand the interfacial micromechanics of fiber reinforced polymer matrix composites more clearly.

- The tensile testing of the microcomposites can be carried out under an optical microscope and hence the crack initiation and propogation can be tracked and correlated. Using this procedure, the energy-release based approach could be used to estimate the local failure criterion for determining fiber-matrix interface strength.

- The physical and mechanical properties of the fluorinated epoxy can be determined and used with the local ultimate interfacial shear strength approach proposed by recent researchers to estimate the interface properties more accurately.

- The fiber-matrix interface traction-separation property can be estimated and used with cohesive zone modeling to characterize more accurately the fiber-matrix debond-

ing phenomena using finite element technique.

- The fiber-matrix surface chemistry can be studied using raman spectroscopy or FTIR techniques to study the changes in interatomic bonding at the fiber-matrix interface.

- The microbond experimental technique can be modified by introducing a pre-existing crack length along the fiber-matrix interface. Exact equations exist based on the fracture mechanics approach. This would form a novel microfracture experiment which would potentially characterize the fiber-matrix interface very accurately.

BIBLIOGRAPHY

[1] K. Campbell, "Airbus to start manufacturing parts for the new A350-XWB in late 09," *Engineering News*, 2009.

[2] M. Hanson, "Production of boeing 787 dreamliners," *Boeing News*.

[3] G. Springer, "Environmental effects on composite materials," vol. 1, 2 and 3, 1984.

[4] B. G. Kumar, R. P. Singh, and T. Nakamura, "Degradation of carbon fiber-reinforced epoxy composites by ultraviolet radiation and condensation," *Journal of Composite Materials*, vol. 36, no. 24, pp. 2713–2733, 2002.

[5] P. Herrerafranco and L. Drzal, "Comparison of methods for the measurement of fiber matrix adhsesion in composites," *Composites*, vol. 23, no. 1, pp. 2–27, 1992.

[6] G. Rao, C. Manas, and N. Balasubramanian, "A fickian diffusion model for permeable fibre polymer composites," *Journal of Reinforced Plastics and Composites*, vol. 2, pp. 289–299, 1992.

[7] S. C. Stuart M Lee, Ronald S Bauer, "Reference book for composite technology," vol. 1, p. 36, 1989.

[8] D. De Renzo, "Advanced composite materials products and manufacturers," p. 1083, 1988.

[9] H.-G. Elias, "An introduction to plastics," p. 319, 1993.

[10] J. Bicerano, "Prediction of polymer properties," *Plastics Engineering*, p. 46, 1993.

[11] W. Institute, "The automotive industry - core research from twi," p. 46, 2000.

[12] A. K. Kulshreshtha, "Handbook of polymer blends and composites," vol. 1, 2002.

[13] P. Geoffrey, "Reinforced plastics durability," p. 372, 1999.

[14] K. Liao, C. Schultheisz, D. Hunston, and L. Brinson, "Long-term durability of fiber-reinforced polymer-matrix composite materials for infrastructure applications: A review," *Journal of Advanced Materials*, vol. 30, no. 4, pp. 3–40, 1998.

[15] F. Jones and P. Geoffrey, "Durability of reinforced plastics in liquid environments,," *Reinforced Plastics Durability*, pp. 70–110, 1999.

[16] Y. Weitsman, "Moisture in composites: Sorption and damage, fatigue of composite materials," pp. 385–429, 1991.

[17] K. Hofer, G. Skaper, L. Bennett, and N. Rao, "Effect of moisture on fatigue and residual strength losses for various composites," *Journal of Reinforced Plastics and Composites*, vol. 6, no. 1, pp. 53–65, 1987.

[18] R. Adams and M. Singh, "The dynamic properties of fibre-reinforced polymers exposed to hot, wet conditions," *Composites Science and Technology*, vol. 56, no. 8, pp. 977–997, 1996.

[19] G. Sala, "Composite degradation due to fluid absorption," *Composites Part B-Engineering*, vol. 31, no. 5, pp. 357–373, 2000.

[20] M. Gibbins and D. Hoffman, "Environmental exposure effects on composite materials for commercial aircraft," *NASA Contractor Report*, vol. 2502, 1982.

[21] W. Bascom, "The surface chemistry of moisture induced composite failure," *Composite Materials*, vol. 6, p. 79, 1974.

[22] D. Adams, "Properties characterisation - mechanical/physical hygrothermal properties test methods," *NASA Contractor Report*, vol. 3607, 1982.

[23] B. Dewimille and A. Bunsell, "Accelerated ageing of a glass fiber-reinforced epoxy resin in water," *Composites*, vol. 14, pp. 35–40, 1983.

[24] D. Jeevan Kumar, A. Singh, and R. Singh, "Accelerated environmental degradation of fiber reinforced composites by boilingwater," *Conference Proceedings of Materials Science and Technology*, 2008.

[25] D. Hayward, E. Hollins, P. Johncock, I. McEwan, R. Pethrick, and E. Pollock, "The cure and diffusion of water in halogen containing epoxy/amine thermosets," *Polymer*, vol. 38, no. 5, pp. 1151–1168, 1997.

[26] Z. Tao, S. Yang, Z. Ge, J. Chen, and L. Fan, "Synthesis and properties of novel fluorinated epoxy resins based on 1,1-bis(4-glycidylesterphenyl)1-(3'-trifluoromethylphenyl)-2,2,2-trifluo roethane," *European Polymer Journal*, vol. 43, no. 2, pp. 550–560, 2007.

[27] J. Ding, Z. Tao, L. Fan, and S. Yang, "Synthesis and properties of fluorinated biphenyl-type epoxy resin," *Journal of Applied Polymer Science*, vol. 113, no. 3, pp. 1429–1437, 2009.

[28] C. Wang and Y. Zuo, "Improvement of surface and moisture resistance of epoxy resins with fluorinated glycidyl ether," *Journal of Applied Polymer Science*, vol. 114, no. 4, pp. 2528–2532, 2009.

[29] T. Twardowski and P. Geil, "A higly fluorinated epoxy-resin.3. behavior in composite and fiber-coating applications," *Journal of Applied Polymer Science*, vol. 42, no. 6, pp. 1721–1726, 1991.

[30] Y. Chong and H. Ohara, "Modification of carbon-fiber surfaces by direct fluorination," *Journal of Fluorine Chemistry*, vol. 57, no. 1-3, pp. 169–175, 1992.

[31] J. Maity, C. Jacob, C. Das, and R. Singh, "Direct fluorination of twaron fiber and investigation of mechanical thermal and morphological properties of high density polyethylene and twaron fiber composites," *Journal of Applied Poymer Science*, vol. 107, no. 6, pp. 3739–3749, 2008.

[32] G. Andreevska and Y. A. Gorbatkina, "Adhesion of polymeric binders to glass fiber," *Product R&D*, vol. 11, no. 1, pp. 24–26, 1972.

[33] L. J. Broutman, "Glass-resin joint strength and their effect on failure mechanisms in reinforced plastics," *Polymer Engineering & Science*, vol. 6, no. 3, pp. 263–272, 1966.

[34] J. Bowling and G. W. Groves, "The debonding and pull-out of ductile wires from a brittle matrix," *Journal of Materials Science*, vol. 14, no. 2, pp. 431–442, 1979.

[35] P. Bartos, "Analysis of pull-out tests on fibres embedded in brittle matrices," *Journal of Materials Science*, vol. 15, no. 12, pp. 3122–3128, 1980.

[36] E. Mader, K. Grundke, H. Jacobasch, and G. Wachinger, "Surface, interphase and composite property relations in fiber-reinforced polymers," *Composites*, vol. 25, no. 7, pp. 739–744, 1994.

[37] S. Deng, L. Ye, and Y. Mai, "Measurement of interfacial shear strength of carbon fibre/epoxy composites using a single fibre pull-out test," *Advanced Ccomposite Materials*, vol. 7, no. 2, pp. 169–182, 1998.

[38] L. Drzal, M. Rich, W. Park, and J. Camping, "A single filament technique for determining interfacial shear strength and failure mode in composite materials," *35th Annual Technical Conference, Reinforced Plastics/Composites Institute*, vol. Paper 20-C, 1980.

[39] L. Dilandro, A. Dibenedetto, and J. Groeger, "The effect of fiber-matrix stress transfer on the strength of fiber-reinforced composite-materials," *Polymer Composites*, vol. 9, no. 3, pp. 209–221, 1988.

[40] N. AN, L. Topoleski, W. Sachse, and S. Phoenix, "An acoustic-emission technique for measuring fiber fragment length distributions in the single-fiber-composite test," *Composites Science and Technology*, vol. 35, no. 1, pp. 13–29, 1989.

[41] V. Rao, P. Herrerafranco, A. Ozzello, and L. Drzal, "A direct comparison of the fragmentation test and the microbond pull-out test for determining the interfacial shear strength," *Journal of Adhesion*, vol. 34, no. 1-4, pp. 65–77, 1991.

[42] J. Figueroa, T. Carney, L. Schadler, and C. Laird, "Micromechanics of single filament composites," *Composites Science and Technology*, vol. 42, no. 1-3, pp. 77–101, 1991.

[43] W. Curtin, "Exact theory of fiber fragmentation in a single-filament composite," *Journal of Materials Science*, vol. 26, no. 19, pp. 5239–5253, 1991.

[44] B. Yavin, H. Gallis, J. Scherf, A. Eitan, and H. Wagner, "Continuous monitoring of the fragmentation phenomenon in single fiber composite-materials," *Polymer Composites*, vol. 12, no. 6, pp. 436–446, 1991.

[45] S. Zhandarov, E. Pisanova, and V. Dovgyalo, "Fragmentation of a single filament during tension in a matrix as a method of determining adhesion," *Mechanics of Composite Materials*, vol. 28, no. 3, pp. 270–286, 1992.

[46] J. Scherf and H. Wagner, "Interpretation of fiber fragmentation in carbon epoxy single-fiber composites - possible fiber-pretension effects," *Polymer Science and Engineering*, vol. 32, no. 4, pp. 298–304, 1992.

[47] H. Liu, Y. Mai, L. Zhou, and L. Ye, "Simulation of the fiber fragmentation process by a fracture-mechanics analysis," *Composites Science and Technology*, vol. 52, no. 2, pp. 253–260, 1994.

[48] P. Feillard, G. Desarmot, and J. Favre, "Theoretical aspects of the fragmentation test," *Composites Science and Technology*, vol. 50, no. 2, pp. 265–279, 1994.

[49] L. Zhou, J. Kim, C. Baillie, and Y. Mai, "Fracture-mechanics analysis of the fiber-fragmentation test," *Journal of Composite Materials*, vol. 29, no. 7, pp. 881–902, 1995.

[50] T. Copponnex, "Analysis and evaluation of the single-fibre fragmentation test," *Composites Science and Technology*, vol. 56, no. 8, pp. 893–909, 1996.

[51] J. Varna, R. Joffe, and L. Berglund, "Interfacial toughness evaluation from the single-fiber fragmentation test," *Composites Science and Technology*, vol. 56, no. 9, pp. 1105–1109, 1996.

[52] D. Tripathi and F. Jones, "Measurement of the load-bearing capability of the fibre/matrix interface by single-fibre fragmentation," *Composites Science and Technology*, vol. 57, no. 8, pp. 925–935, 1997.

[53] S. Lee, T. Nguyen, J. Chin, and T. Chuang, "Analysis of the single-fiber fragmentation test," *Journal of Materials Science*, vol. 33, no. 21, pp. 5221–5228, 1998.

[54] C. Hui, D. Shia, and L. Berglund, "Estimation of interfacial shear strength: an application of a new statistical theory for single fiber composite test," *Composites Science and Technology*, vol. 59, no. 13, pp. 2037–2046, 1999.

[55] J. Andersons, R. Joffe, M. Hojo, and S. Ochiai, "Fibre fragment distribution in a single-fibre composite tension test," *Composites Part B-Engineering*, vol. 32, no. 4, pp. 323–332, 2001.

[56] B. Kim and J. Nairn, "Observations of fiber fracture and interfacial debonding phenomena using the fragmentation test in single fiber composites," *Journal of Composite Materials*, vol. 36, no. 15, pp. 1825–1858, 2002.

[57] C. Santulli, "Critical length measurements in carbon fibers during single fiber fragmentation tests using acoustic emission," *Journal of Materials Science*, vol. 39, no. 8, pp. 2905–2907, 2004.

[58] N. Wadswort and I. Spilling, "Load transfer from broken fibers in composite materials," *Journal of Physics D-Applied Physics*, vol. 1, no. 8, pp. 1049–&, 1968.

[59] J. Mandell, J. Chen, and F. McGarry, "A microdebonding test for in situ assessment of fibre/matrix bond strength in composite materials," *International Journal of Adhesion and Adhesives*, vol. 1, no. 1, pp. 40–44, 1980.

[60] B. Miller, P. Muri, and L. Rebenfeld, "A microbond method for determination of the shear strength of a fiber-resin interface," *Composites Science and Technology*, vol. 28, no. 1, pp. 17–32, 1987.

[61] U. Gaur and B. Miller, "Microbond method for determination of the shear-strength of a fiber resin interface - evaluation of experimental parameters," *Composites Science and Technology*, vol. 34, no. 1, pp. 35–51, 1989.

[62] D. Biro, P. Mclean, and Y. Deslandes, "Application of the microbond technique - characterization of carbon-fiber epoxy interfaces," *Polymer Engineering and Science*, vol. 31, no. 17, pp. 1250–1256, 1991.

[63] D. Biro, G. PleiIzier, and Y. Deslandes, "Application of the microbond technique - effects of hygrothermal exposure on carbon-fiber epoxy interfaces," *Composites Science and Technology*, vol. 46, no. 3, pp. 293–301, 1993.

[64] R. Scheer and J. Nairn, "A comparison of several fracture mechanics methods for measuring interfacial toughness with microbond tests," *Journal of Adhesion*, vol. 53, no. 1-2, pp. 45–68, 1995.

[65] R. Day and J. Rodrigez, "Investigation of the micromechanics of the microbond test," *Composites Science and Technolofy*, vol. 58, no. 6, pp. 907–914, 1998.

[66] T. Schuller, U. Bahr, W. Beckert, and B. Lauke, "Fracture mechanics analysis of the microbond test," *Composites Part A-Applied Science and Manufacturing*, vol. 29, no. 9-10, pp. 1083–1089, 1998.

[67] H. Kessler, T. Schuller, W. Beckert, and B. Lauke, "A fracture-mechanics model of the microbond test with interface friction," *Composites Science and Technology*, vol. 59, no. 15, pp. 2231–2242, 1999.

[68] C. Liu and J. Nairn, "Analytical and experimental methods for a fracture mechanics interpretation of the microbond test including the effects of friction and thermal stresses," *International Journal of Adhesion and Adhesives*, vol. 19, no. 1, pp. 59–70, 1999.

[69] J. Nairn, "Fracture mechanics of composites with residual stresses, imperfect interfaces, and traction-loaded cracks," *Composites Science and Technology*, vol. 61, no. 15, pp. 2159–2167, 2001.

[70] E. Pisanova, S. Zhandarov, and E. Mader, "How can adhesion be determined from micromechanical tests?," *Composites Part A-Applied Science and Manufacturing*, vol. 32, no. 3-4, pp. 425–434, 2001.

[71] A. Towo, M. Ansell, M. Pastor, and D. Packham, "Weibull analysis of microbond shear strength at sisal fibre-polyester resin interfaces," *Composite Interfaces*, vol. 12, no. 1-2, pp. 77–93, 2005.

[72] L. Drzal, N. Suguira, and D. Hook, "The role of chemical bonding and surface topography in adhesion between carbon fibers and epoxy matrices," *Composite Interfaces*, vol. 4, pp. 337–354, 1997.

[73] Y. Gorbatkina, "Adhesive strength of fiber-polymer systems," 1992.

[74] L. DiLandro and M. Pegoraro, "Evaluation of residual stresses and adhesion in polymer composites," *Composites Part A - Applied Science and Manufacturing*, vol. 27, no. 9, pp. 847–853, 1996.

[75] P. Herrerafranco, V. Rao, L. Drzal, and M. Chiang, "Bond strength measurement in composites - analysis of experimental-techniques," *Composites Engineering*, vol. 2, no. 1, pp. 31–45, 1992.

[76] S. Park and T. Kim, "Studies on surface energetics of glass fabrics in an unsaturated polyester matrix system: effect of sizing treatment on glass fabrics," *Journal of Applied Poymer Science*, vol. 80, pp. 1439–1445, 2001.

[77] S. Keusch, H. Queck, and K. Gliesche, "Influence of glass fibre epoxy resin interface on static mechanical properties of unidirectional composites and on fatigue performance of cross ply composites," *Composites Part A-Applied Science and Manufacturing*, vol. 29, no. 5-6, pp. 701–705, 1998.

[78] S. Keusch and R. Haessler, "Influence of surface treatment of glass fibres on the dynamic mechanical properties of epoxy resin composites," *Composites Part A-Applied Science and Manufacturing*, vol. 30, no. 8, pp. 997–1002, 1999.

[79] C. Baley, Y. Grohens, F. Busnel, and P. Davies, "Application of interlaminar tests to marine composites. relation between glass fibre/polymer interfaces and interlaminar properties of marine composites," *Applied Composite Materials*, vol. 11, no. 2, pp. 77–98, 2004.

[80] P. Mallick, "Composites engineering handbook, issue 14702," *Materials Engineering*, vol. 11, p. 121, 1997.

[81] R. B. Durairaj, "Resorcinol: chemistry, technology and applications," p. 748, 2005.

[82] J. Hinkley, "Private communication," 2007.

[83] H. Corporation, "Hextow im7 carbon fibers," *HexTow IM7 Product Sheet*, 2009.

[84] B. Carroll, "Equilibrium conformations of liquid-drops on thin cylinders under forces of capillarity - a theory for the roll-up process," *Langmuir*, vol. 2, no. 2, pp. 248–250, 1986.

[85] J. Ash, W. Cross, D. Svalstad, J. Kellar, and L. Kjerengtroen, "Finite element evaluation of the microbond test: meniscus effect, interphase region, and vise angle," *Composites Science and Technology*, vol. 63, no. 5, pp. 641–651, 2003.

[86] M. Nishikawa, T. Okabe, K. Hemmi, and N. Takeda, "Micromechanical modeling of the microbond test to quantify the interfacial properties of fiber-reinforced composites," *International Journal of Solids and Structures*, vol. 45, no. 14-15, pp. 4098–4113, 2008.

[87] H. S. Chemicals, "Epon 862/epikure 3234 technical data sheet inc," 2008.

VITA

Chirag H. Kareliya

Candidate for the Degree of

Master of Science

Thesis: INTERFACIAL MICROMECHANICS AND EFFECT OF MOISTURE ON FLUORINATED EPOXY CARBON FIBER COMPOSITES

Major Field: Mechanical Engineering

Biographical:

Personal Data: Born in Mumbai, India on August 9th, 1982.

Education:

Received the B.E. degree from Rizvi College of Engineering of University of Mumbai, Mumbai, India, 2005, in Mechanical Engineering
Completed the requirements for the degree of Master of Science with a major in Mechanical Engineering Oklahoma State University in December, 2009.

Experience:

Worked as a Graduate Research Assistant at the Mechanics of Advanced Materials Laboratory headed by Dr. Raman P. Singh in the area of polymer reinforced composites

Name: Chirag H. Kareliya Date of Degree: December, 2009

Institution: Oklahoma State University Location: Stillwater, Oklahoma

Title of Study: INTERFACIAL MICROMECHANICS AND EFFECT OF MOISTURE ON FLUORINATED EPOXY CARBON FIBER COMPOSITES

Pages in Study: 50 Candidate for the Degree of Master of Science

Major Field: Mechanical Engineering

Carbon fiber composites have witnessed an increased application in aerospace and other civil structures due to their excellent structural properties like specific strength and stiffness. For example, the Airbus A350 XWB contains 53% composites whereas the Boeing 787 Dreamliner contains 50% composites by weight. Unlike other structural materials like Steel and Aluminum, Carbon fiber composites have not been as widely studied and hence, their increased application is also accompanied with a serious concern about their long-term durability. Many of these applications are exposed to multiple environments like moisture, temperature and UV radiation. Composites based on conventional epoxies readily absorb moisture. However, scientists at NASA LaRC have synthesized novel fluorinated epoxies, which show reduced moisture absorption and hence potentially better long term durability. The aim of this project is to study the effect of moisture absorption on fluorinated-epoxy based carbon fiber composites and its comparison with conventional epoxy carbon fiber based composites. Microbond tests are currently being performed on fluorinated and non-fluorinated epoxy based single fiber samples before and after boiling water degradation. It is expected that fluorinated epoxy based single fiber coupons will show relatively reduced degradation of interface as compared to the non-fluorinated epoxy single fiber coupons.

ADVISOR'S APPROVAL: _____